Food Chemistry: X 23 (2024) 101724

Contents lists available at ScienceDirect

Food Chemistry: X

journal homepage: www.sciencedirect.com/journal/food-chemistry-x

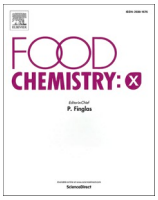

Improvement of NaCas/DGMO complex emulsion on resveratrol stability, *in vitro* bioaccessibility, *in vivo* bioavailability and gut microbiota

Hong Lin [a,b,c,*], Huan Chen [a], Siqi Wang [a], Junbo He [a,b,c], Weinong Zhang [a,b,c,*]

[a] *Wuhan Polytechnic University, School of Food Science and Engineering, China*
[b] *Hubei Key Laboratory for Processing and Transformation of Agricultural Products (Wuhan Polytechnic University), China*
[c] *MOE Key Laboratory for Deep Processing of Major Grain and Oil (Wuhan Polytechnic University), China*

ARTICLE INFO

Keywords:
Resveratrol
Emulsions
Bioavailability
Gut microbiota

ABSTRACT

Evaluation for biological impact of food emulsions is fundamental for their application. In present study, we utilized a NaCas-DGMO (sodium caseinate-decylglycerol monooleate) stabilized emulsion to improve resveratrol's (Res) stability, and bioavailability. The *in vivo* interaction between complex emulsion and gut microbiota was further explored. Results indicated NaCas-DGMO emulsion achieved a loading rate of 92 % for Res and significantly enhanced storage and photo stability of Res. *In vitro* gastrointestinal digestion highlighted a significant improvement in Res's bioaccessibility. *In vivo* pharmacokinetic tests showed a notable 3.1-fold increase in oral bioavailability, with a prolonged T_{max} of 6 h post-administration. Gut microbiota analysis revealed that the emulsion promoted beneficial bacteria, like *Blautia*, which produce short-chain fatty acids. Consequently, the findings proved potential of NaCas-DGMO stabled emulsion as carriers for bioactive substances in the food industry. The innovative methodology employed in assessing biological effects provides valuable insights for future research in related field.

1. Introduction

The application of food-grade emulsions loaded with active ingredients to food is a rapidly developing area of interest within the food industry (Ghorbanzade, Jafari, Akhavan, & Hadavi, 2017; Shang et al., 2020). It could enhance the stability of active compounds, promote their bioavailability, improve the flavor and texture of food products, and extend the shelf life of foodstuffs (Sahraeian, Rashidinejad, & Golmakani, 2024; Shi, Chen, He, Zhang, & Lin, 2024). The related products exhibit considerable potential for application and commercialization. As a case in point, resveratrol (Res)—a plant-derived polyphenol—has been demonstrated to exhibit a range of pharmacological effects, including antioxidant, anti-inflammatory, anti-cardiovascular disease, anti-cancer, and anti-DNA damage properties (Mora-Gutierrez, Attaie, de Gonzalez, Jung, & Marquez, 2020; Wenzel, Soldo, Erbersdobler, & Somoza, 2005). However, its poor water solubility and susceptibility to oxidative degradation or photolysis during food processing and storage limit its bioavailability when taken orally (Andres-Lacueva et al., 2012; Dima, Assadpour, Dima, & Jafari, 2020). A common solution is to use nanoemulsions to load Res to improve the bioavailability of the latter (Sahraeian et al., 2024; Silva et al., 2023). Li Wang et al. employed casein nanoparticles stabled emulsion improved the oral bioavailability of apigenin by 3 times compared to the raw apigenin(Wang, Jia, Yang, Cai, & Zhao, 2024). Gausuzzaman et al. utilized self-emulsion drug delivery system (SEDDS) for resveratrol. The optimized SEDDS formulation resulted in a 48-fold enhancement in bioavailability compared to pure resveratrol(Gausuzzaman et al., 2022). Thus, the quality and characteristics of the nanoemulsion determine the bioavailability of the loading compounds.

Recently, researchers have mostly evaluated the quality and properties of emulsions in terms of micro/macro morphological characterization of the nanoemulsion systems and the stability of the emulsion systems under different conditions (Mora-Gutierrez et al., 2020; Sessa et al., 2014). Accordingly, a variety of emulsion systems (including protein-based approaches (Lin, Fu, Hu, Zhang, & He, 2024; Yin, Dong, Cheng, Ji, & Liang, 2022), polysaccharides (Liu et al., 2023), self-emulsifying micelles/ hydrogel composite (Joseph, Balakrishnan, Shanmughan, Maliakel, & Illathu Madhavamenon, 2022), protein-small-molecule surfactant conjugates/complexes (Zhu et al., 2021) (Murray, 2002)) have been demonstrated to be effective in improving the solubility of a range of compounds. The group of Rebeca Peñalva reported that Res loaded in casein nanoparticles has an oral bioavailability of

* Corresponding author at: Wuhan Polytechnic University, China.
E-mail address: linhong@whpu.edu.cn (H. Lin).

https://doi.org/10.1016/j.fochx.2024.101724
Received 2 July 2024; Received in revised form 8 August 2024; Accepted 9 August 2024
Available online 10 August 2024

26.5 %, which is 10 times higher than when Res is administered as an oral solution (Peñalva et al., 2018)(Table 1). The emulsion system was found to be highly effective in improving bioavailability of Res. Furthermore, *in vitro* studies simulating gastrointestinal digestion and Caco-2 cell models demonstrated that the nanoemulsion system could effectively control the release of Res and enhance its bioavailability (Ai, Fang, Zhang, & Liao, 2022; Hu et al., 2023). The findings of these studies provided a foundation for the application of food emulsions with the aim of enhancing their bioavailability (Table 1).

Actually, nanoemulsions were digested in the intestines after passing through the stomach. The digestion of food in the body involved not only intestinal absorption but also a dynamic metabolic process. Therefore, the evaluation of food-grade emulsions loaded with active ingredients depends not only on *in vitro* or simulated digestion experiments, but also *in vivo* experiments, to further comprehensively characterize their efficacy and applicability. The interaction between food and intestinal flora exerts a substantial influence on a range of physiological processes (Wu et al., 2019), including digestion, metabolism, and the modulation of the host's immune system (Nicholson et al., 2012). These interactions have a subsequent impact on the host's benefits. Therefore, a combination of *in vitro* and *in vivo* experiments is necessary to fully evaluate the applicability of emulsions in the food field. These experiments should monitor the bioavailability of the active ingredients and focus on the response mechanisms of the intestinal metabolism *in vivo*. It would provide the necessary biological data for the application of food grade emulsions.

Our previous studies have reported that sodium caseinate (NaCas) and DGMO (Decaglycerol Monooleate) could self-assemble in an aqueous medium to generate emulsions suitable for food products (CHENG Yingxue, Menglu, & Junbo, 2022). The present study focuses on the effect of the NaCas-DGMO complex emulsion on intestine. The emulsion properties and stability of NaCas-DGMO binary complexes of Res-rice bran oil emulsions were characterized. The digestive behavior of Res complex emulsions in simulated gastrointestinal fluids and *in vivo* intestinal tracts were explored. The *in vitro* dynamic bioaccessibility and *in vivo* bioavailability of Res were also investigated. Furthermore, we examined the modification of community structure of intestinal microbiome induced by emulsion system. The study innovatively explores the regulatory mechanisms of Res-loaded NaCas-DGMO nanoemulsion on the intestinal flora of SD (Sprague-Dawley) rats. Moreover, the strategy of integrating *in vitro* simulations with *in vivo* animal experiments to investigate the biological effects of nanoemulsions, as proposed in this study, serves as a reference for similar research endeavors. Our findings contribute crucial foundational data for the prospective application of emulsion systems within the food industry.

Table 1
A summary of previously published studies about active compound-delivery and their biological effect evaluation.

Author	Year	Delivery and Active Compound	Improvement of Bioavailability	Biological Effect Evaluation
Peñalva et al. (2018)	2018	Casein nanoparticles for resveratrol	The encapsulation of resveratrol in casein nanoparticles resulted in a 26.5 % relative oral bioavailability, which was 10 times higher than the oral solution of resveratrol.	The sustained plasma levels of resveratrol and its major metabolite were observed for at least 8 h.
Gausuzzaman et al. (2022)	2022	Self-Emulsifying Drug Delivery System (SEDDS) for resveratrol	The optimized SEDDS formulation resulted in a 48-fold enhancement in bioavailability compared to pure resveratrol.	*In vivo* pharmacokinetic study in rats
Wang et al. (2024)	2024	Casein nanoparticles for the delivery of apigenin	The oral bioavailability of apigenin was improved by 3 times compared to the raw apigenin	*In vivo* pharmacokinetic studies; Gastrointestinal stability and hypoglycemic activity

2. Materials and methods

2.1. Materials

Res (Resveratrol, Trans-isomer, purity ≥98.0 %), NaCas (Casein sodium salt, from bovine milk), Nile Red and fluorescein isothiocyanate (FITC) were purchased from Sigma Aldrich Co. (St. Louis, MO, USA). Decaglycerol Monooleate (DGMO), characterized by an HLB value of 12.9 and designated as food-grade quality, was acquired from Shandong Binzhou GIN&ING New Material Technology Co., Ltd. (Bingzhou, China). The rice bran oil was bought from a local supermarket in Wuhan, China. For enzyme preparations, pepsin from porcine gastric mucosa (P7125, >400 units/mg protein), bile extracts porcine (B8631), and pancreatin from porcine pancreas (P3292, meeting 4*USP specifications) were all sourced from Sigma-Aldrich (MO, USA). Methanol of HPLC grade was procured from Fisher Scientific (NJ, USA), and Milli-Q water (Millipore, Bedford, MA) served as our primary solvent throughout the study. All other chemicals, reagents, and solvents were obtained from Sinopharm Chemical Reagent Co., Ltd. (Shanghai, China) and were of analytical grade or higher.

2.2. Preparation of Res-loaded NaCas-DGMO emulsions

The fabrication of NaCas-DGMO complex dispersion followed a previously reported method with minor modifications, as described in our earlier publication (CHENG Yingxue et al., 2022; Shi, Chen, et al., 2024). The pH of the stock solutions was adjusted to 7 by the addition of 0.1 mol/L HCl solution. To obtain the NaCas-DGMO complex dispersion ($w/w = 1$), 100 mL of NaCas stock solution was mixed with 100 mL of DGMO stock solution, followed by stirring for 1 h at room temperature. To prevent microbial growth, 0.01 % (w/v) sodium azide was added to the dispersion. The particle size, polydispersity index (PDI), micromorphology, physical properties, and stability data of the NaCas-DGMO complex dispersion were previously reported in our earlier paper. (CHENG Yingxue et al., 2022).

The preparation of the oily phase involved the following well-defined steps: Initially, a stock solution of Res, with a concentration of 22 mg/mL, was meticulously prepared in ethanol. Subsequently, 1 mL of this Res solution was individually mixed with 2 g and 4 g of rice bran oil, respectively. These mixtures were subjected to stirring for 30 min at 85 °C to facilitate the complete evaporation of ethanol. Importantly, it should be noted that the density of rice bran oil (about 0.9 g/mL) is lower than that of water (1 g/mL). For the creation of the Res-loaded NaCas-DGMO emulsion, with a targeted 5 % oil weight proportion, precisely 41.8 mL of the NaCas-DGMO dispersion was combined with 2 g of the Res oily phase. Subsequently, this mixture underwent homogenization at 8000 rpm for 1 min, utilizing a high-speed blender (XHF-DY, Ningbo Xinzhi Tech. Co., Ningbo, China). Following this initial homogenization step, the resulting emulsion was subjected to further enhancement through three additional homogenization cycles. This process was carried out using a Nano DeBEE30–4 high-pressure homogenizer (Nano Debe, USA) operating at a pressure of 10,000 psi.

Similarly, the 10 % oil (w/w) Res-loaded emulsion was prepared

following the identical procedure, except that 39.6 mL of NaCas-DGMO dispersion was blended with 4 g of the Res oily phase. The final volume and concentration of Res in the two groups of complex emulsions were kept constant. Control samples were prepared for comparative analysis, including high-speed high-pressure homogenization-treated emulsions devoid of Res, Res-loaded complex dispersions lacking oil, and Res/NaCas/DGMO suspension.

2.3. Confocal laser scanning microscopy (CLSM)

The dispersion and interfacial structure of emulsion and digesta droplets were observed with CLSM (FV10, Olympus, Japan) through the previously described method (Zhu et al., 2021). Briefly, 1 mL samples were mixed with 300 μL Nile red (0.01 mg/mL) and 300 μL FITC (0.01 mg/mL). After vortex mixing, the samples were stored for 12 h away from light. Then, 10 μL mixtures were deposited on concave confocal microscope slides with a coverslip covered. The protein particles and oil droplets were dyed with FITC (excitation with a helium-neon laser at 543 nm) and Nile red (excitation with an argon krypton laser at 488 nm), respectively. The resolution of the objective lens was set at 40×.

2.4. Effect of pH, ionic strength, and temperature on emulsion stability

The impact of environmental conditions was assessed through several parameters, including the *Z*-average mean diameter and polydispersity index (PDI), employing a Zetasizer Nano ZS90 instrument (Malvern Instruments Ltd., Worcestershire, UK).

pH The pH levels of Res-loaded emulsions containing 5 % and 10 % oil were adjusted to specific values of 2.0, 3.0, 6.0, and 7.0, utilizing either sodium hydroxide (NaOH) or hydrochloric acid (HCl). The particle size and PDI of the emulsions were determined following an equilibration of 30 min.

Ionic Strength The freshly prepared 5 % and 10 % oil Res-loaded emulsions were mixed with varying amounts of NaCl powder and stirred until completely dissolved. The final NaCl concentrations in the different emulsions were adjusted to 10, 25, 50, 100, 200, 300, 400, and 500 mM. After an incubation of 30 min, the droplet size and polydispersity index (PDI) of the emulsions were measured.

Temperature The freshly prepared 5 % oil and 10 % oil Res-loaded emulsions were subjected to a controlled temperature in a water bath at temperatures of 40, 50, and 60 °C, maintained for a 30-min duration. Following this incubation period, the emulsions were cooled down to 25 °C and settled for an additional 30 min. Subsequently, the droplet size and polydispersity index (PDI) were measured.

Storage Stability Two groups of emulsions loaded with Res and containing 5 % and 10 % oil, respectively, were prepared and stored. The first group was stored in a refrigerator set at 4 °C, while the second group was stored in a thermostatic chamber at 25 °C. The droplet size and PDI were recorded.

2.5. Measurement of the encapsulation efficiency (EE)

The Res-loaded NaCas-DGMO emulsions were subjected to centrifugation at 10,000 rpm for 30 min using an ultracentrifuge (H1750, Xiangyi Li. Co., Changsha, China). The resulting supernatants were subsequently diluted 50-fold with ethanol to facilitate the quantification of encapsulated Res. The diluted samples underwent ultrasonic extraction for 30 min, followed by centrifugation at 3000 rpm for 10 min. The quantification of Res was performed using an Agilent 1260 Infinity HPLC system (Agilent Technologies, Inc., Santa Clara, United States). To establish the standard calibration curve, a series of Res concentration standard solutions were meticulously prepared in ethanol. Chromatographic separation was accomplished utilizing a Venusil XB C18 column (150 mm × 4.6 mm, 5 μm). The mobile phase employed consisted of an isocratic elution comprising 40 % acetonitrile and 60 % purified water (*v*/v). The column temperature was precisely maintained at 25 °C, with a constant flow rate of 1 mL/min. For the quantification of Res, the detection wavelength was set at 306 nm. The encapsulation efficiency (EE) of Res was calculated using the following eqs. (1):

$$EE(\%) = \frac{mass\ of\ encapsulated\ Res(mg)}{total\ mass\ of\ Res\ added\ in\ encapsulation(mg)} \times 100 \quad (1)$$

2.6. Transmission electron microscopy (TEM)

The 10 % oil Res-loaded emulsion, along with a NaCas solution used as a control, were subjected to further characterization using transmission electron microscopy (TEM). For TEM imaging, the diluted samples were carefully placed on a 400-mesh copper grid and subsequently stained with 2 % uranyl acetate for a duration of 2 min. The stained samples were then imaged using a HT7700 TEM instrument (HITACHI, Japan) operating at an acceleration voltage of 80 kV.

2.7. The effect of light on the retention rates of Res in emulsions for 21-day storage

A fresh 0.5 mg/mL Res-loaded NaCas-DGMO emulsion (referred to as RE) containing 10 % oil (v%) was prepared. In parallel, a corresponding Res/NaCas/DGMO/oil suspension (designated as RC), containing 10 % oil but not having undergone high-speed high-pressure treatment, was formulated. Additionally, solutions with an equal Res concentration in both aqueous form (referred to as saline, RW) and oil form (using rice bran oil, designated as RO) were prepared. Each of these samples was systematically divided into two equal portions. One portion was transferred into transparent glass vials and exposed to ambient light conditions, while the other portion was placed within brown vials and covered with aluminum foil, thus simulating a dark environment.

The experiment was carried out over a period of 21 days, with measurements of Res retention rate being recorded at 7-day intervals. The objective of this retention rate measurement was to evaluate the stability and long-term resilience of Res within the different sample formulations over time.

The measurement of Res-retention rate 50 μL samples were diluted 50-fold with anhydrous ethanol. The resulting mixture underwent ultrasonic treatment at 50 kHz and 25 °C for 30 min to ensure the complete release of Res from emulsion droplets. Following this, the mixture was subjected to centrifugation at 3000 rpm for 20 min, and the resulting supernatant was filtered through a 0.22 μm organic phase filter. Subsequently, the concentration of Res in the filtered supernatant was determined using high-performance liquid chromatography (HPLC) and denoted as 'C.' The Res concentration of the newly prepared sample was expressed as 'C_0.' The retention rate was calculated as Eqs. (2):

$$Retention\ rate\ (\%) = \frac{C}{C_0} \times 100 \quad (2)$$

2.8. In vitro simulated gastrointestinal digestions

Four sample groups (RE, RC, RW, RO) were freshly prepared to investigate the digestion behavior and bioaccessibility of Res during *in vitro* digestion using simulated gastric fluid (SGF) and simulated intestinal fluid (SIF), following a previously reported method(Huang et al., 2020). The Res concentration in all four groups of samples was standardized.

The SGF (pH 2.0) was prepared by combining 3.2 mg/mL pepsin with 0.15 M NaCl. During the gastric digestion stage, 10 mL of each sample was mixed with an equivalent volume of SGF and incubated at 37 °C for 2 h with continuous stirring. Subsequently, the pH of the resulting 20 mL digesta was adjusted to 7.0 to simulate intestinal digestion. The digesta was then mixed with 20 mL of SIF, comprising 10 mg/mL bile salts, 1 mg/mL pancreatin, and 10 mM $CaCl_2$. This mixture was incubated at 37 °C for 4 h.

During the gastric digestion phase, 200 μL of samples were collected at 0 min, 10 min, 20 min, 30 min, 60 min, and 120 min. For the intestinal digestion phase, samples were collected at 0 min, 10 min, 20 min, 30 min, 60 min, 120 min, 180 min, and 240 min. At each collection time point, the samples were supplemented with an equal equivalent of SGF or SIF, depending on the corresponding stage of digestion.

The bioaccessibility of Res The bioaccessibility of Res was evaluated by determining the solubilized Res in mixed micelles, which represents the *in vitro* bioaccessible fraction of Res in gastrointestinal fluid. To separate the mixed micelle layer, the collected digesta samples obtained at different time intervals during the digestion phase were centrifuged at 12,000 rpm for 30 min at 4 °C, utilizing an H1750 centrifuge (Xiangyi Li. Co., Changsha, China). Subsequently, the mixed micelle fraction was diluted with acetonitrile and subjected to centrifugation at 8000 rpm for 3 min. The resulting supernatants were then filtered through a 0.22 μm syringe filter. The quantification of Res was carried out using high-performance liquid chromatography (HPLC), as outlined in Section 2.3.

The *in vitro* bioaccessibility of Res was calculated using the following eq. (3):

$$Bioaccessibility\ (\%) = \frac{cumulative\ amount\ of\ Res\ in\ mixed\ micelles}{amount\ of\ Res\ before\ digestion} \times 100 \quad (3)$$

2.9. In vivo animal experiment

Animal experiment design Twenty-eight male specific pathogen-free (SPF) SD rats, aged 8 weeks, were obtained from Hubei Beiente Biotechnology Co., Ltd. (Permission number: 110324210106340764) The rats were housed in a suitable facility and provided with standard chow and water *ad libitum*. After a two-week acclimatization period under SPF conditions, with a temperature maintained at 24 ± 0.5 °C and a relative humidity of 50–60 %, the rats were randomly divided into four groups ($n = 7$). RE-treated, RC-treated, RW-treated, and RO-treated. The study involved four groups of rats. Each group received intragastric administration of a 0.5 mg/mL Res-loaded emulsion (RE), 0.5 mg/mL Res-loaded coarse emulsion (RC), 0.5 mg/mL Res's saline (RW), and 0.5 mg/mL Res oily (RO) solution, respectively, following a 12-h fasting period. This study received animals and protocols approval from the Animal Research Ethics Application at the Wuhan Polytechnic University and followed the national ethical guidelines for laboratory animals.

Samples collection Baseline blood samples were extracted from the rats' tail vein at the 0-h time point before any administration. Subsequent blood samples were collected at predefined time intervals of 0.5, 1, 2, 4-, 6-, 8-, and 12-h post-administration. All collected blood was transferred into heparinized centrifuge tubes and subjected to centrifugation at 10,000 rpm for 15 min at 4 °C to isolate serum. Subsequently, all animals were humanely euthanized using carbon dioxide asphyxiation followed by cervical dislocation at 0.5 h after blood collection. In addition to blood samples, the contents of the small intestine, cecum, and colon were collected for further analysis. All bio-samples were preserved at −80 °C until subsequent analyses.

Sample preparation 50 μL of serum was mixed with 150 μL of acetonitrile and vortexed for 3 min. The protein was removed by centrifugation at 10,000 rpm for 10 min using a high-speed centrifuge. Then, 30 μL of the supernatant was collected for Res-quantitative HPLC analysis. For the intestinal content, 15 mg was mixed with 100 μL of acetonitrile and homogenized for 1 min. The mixtures were centrifuged at 10,000 rpm for 10 min, and the supernatant was selectively collected for Resveratrol quantification *via* HPLC analysis.

2.10. Colonic microbiota profiling

Intestinal bacterial DNA were extracted from colonic content using an E.Z.N.A. Stool DNA Kit (D4015, Omega, Inc.) under the instructions. PCR Amplification and Pyrosequencing were entrusted Shanghai Majorbio Bio-pharm Technology Co.,Ltd. DNA were amplified with 338F (5′- ACTCCTACGGGAGGCAGCAG-3′) as forward primer and 806R (5′- GGACTACHVGGGTWTCTAAT-3′) as the reverse primer specifically for V3 - V4 regions of the 16S rRNA. The libraries were sequenced and performed on the MiSeq PE 250 platform. Bioinformatic analysis were carried out as our previous report (Lin, An, Hao, Wang, & Tang, 2016).

2.11. Statistical analysis

All experiments were performed in triplicate at least. Statistical analysis was conducted using SPSS software (IBM SPSS statistic 19). The significant level (p) was set at 0.05. The data were displayed as mean ± standard deviation (SD), and plotted using OriginPro 2021 (OriginLab, Northampton, MA 01060 UNITED STATES). The pyrosequencing data was plotted with R package.

3. Results and disscussion

3.1. The CLSM of Res-loaded NaCas-DGMO emulsions

Based on our previous research, NaCas-DGMO nanoparticle showed favorable performance in stabilizing emulsions. In this study, the application and the biological of NaCas-DGMO nanoparticle in Res's delivery was explored and evaluated. To characterize the Res-loaded complex emulsions, the microstructure of the Res-loaded NaCas-DGMO complex nanoemulsion was observed using CLSM. As depicted in Fig. 1, oil droplets stained red by Nile Red and sodium caseinate stained green by FITC in Res emulsion system. From Fig. 1, it was observed that oil droplets were dispersed in emulsion system in all of three groups, that is, 5 % oil NaCas-DGMO emulsion, 0.5 mg/mL Res-loaded NaCas-DGMO emulsion with 5 % oil (v%) and 0.5 mg/mL Res-loaded NaCas-DGMO emulsion with 10 % oil (Fig. 1A, C, E). Notably, the addition of Res into the complex emulsion exerts minimal influence on droplet dispersion, as demonstrated in the comparison of Fig. 1C with Fig. 1A. Moreover, the dispersion of droplets in the Res-loaded 10 %-oil emulsion is remarkably uniform. Under higher magnification, as depicted in Fig. 1B, D and E, it is apparent that the dispersed droplets assume a spherical configuration, with the red-stained oily droplets enveloped by the green-stained NaCas-DGMO complex. Therefore, three emulsion groups were oil-in-water

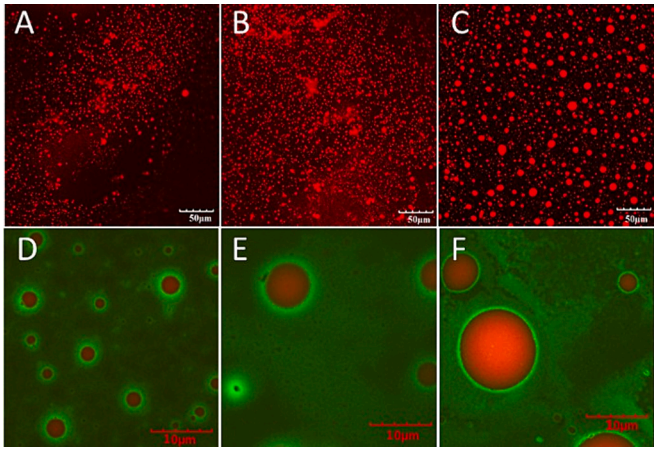

Fig. 1. Confocal laser scanning microscopy (CLSM) images of (A, D) 5 % oil (v %), (B, E) 0.5 mg/mL of Res-loaded 5 % oil (v%), and (C, F) 0.5 mg/mL of Res-loaded 10 % oil (v%) NaCas-DGMO emulsions. The oil droplets stained red by Nile Red and sodium caseinate was not stained in A-C; The oil droplets stained red by Nile Red and sodium caseinate stained green by FITC in D—F. The measurements were repeated three times. (For interpretation of the references to colour in this figure legend, the reader is referred to the web version of this article.)

emulsions. Furthermore, the droplet size of the Res-loaded 5 % oil emulsion was smaller compared to that of the 10 % oil emulsion, indicating that droplet size within the Res complex emulsion scales proportionally with the oil phase content. The results of the laser confocal observations are consistent with previous particle size measurements (CHENG Yingxue et al., 2022). Comparatively, the NaCas-HGMO (hexaglycerol monooleate) complex was reported had good effect on stabilization of O/W emulsions that loaded curcumin (Shi et al., 2024). The results also supported our findings.

3.2. The pH, ionic strength, temperature and storage stability of Res-loaded NaCas-DGMO complex emulsion.

The pH value has been an important environmental factor in the practical application of food emulsions, as it significantly influences their stability and functional properties. Here, the pH stability of Res-loaded complex emulsion was evaluated, with particle size and polydispersity index (PDI) as indicators. Res-loaded NaCas emulsions (5 % and 10 % oil content) were used as the control groups. As illustrated in Fig. 2A, the incorporation of DGMO to NaCas narrowed down the particle size range of the Res-loaded emulsions at pH 2, 3, 6, 7 from 262.0 ± 1.34 nm ~533.8 ± 7.49 nm to 248.4 ± 4.12 nm ~ 382.1 ± 1.68 nm. It suggested that the combination of DGMO to NaCas mitigated the pH-dependent variations in the particle size distribution of Res-loaded emulsions. PDI serves as an essential indicator for assessing the uniformity of size distribution, with values below 0.3 indicating a more uniform distribution (Tamjidi, Shahedi, Varshosaz, & Nasirpour, 2013). The Res-loaded complexes had lower particle size and PDI under all pH conditions, including pH 2, 3, 6 and 7, compared to the NaCas-groups. It probably ascribed to that the increased surface hydrophobicity of NaCas-DGMO complex nanoparticle improved the dispersion of emulsion (Acharya, Sanguansri, & Augustin, 2013; Chen et al., 2023; CHENG

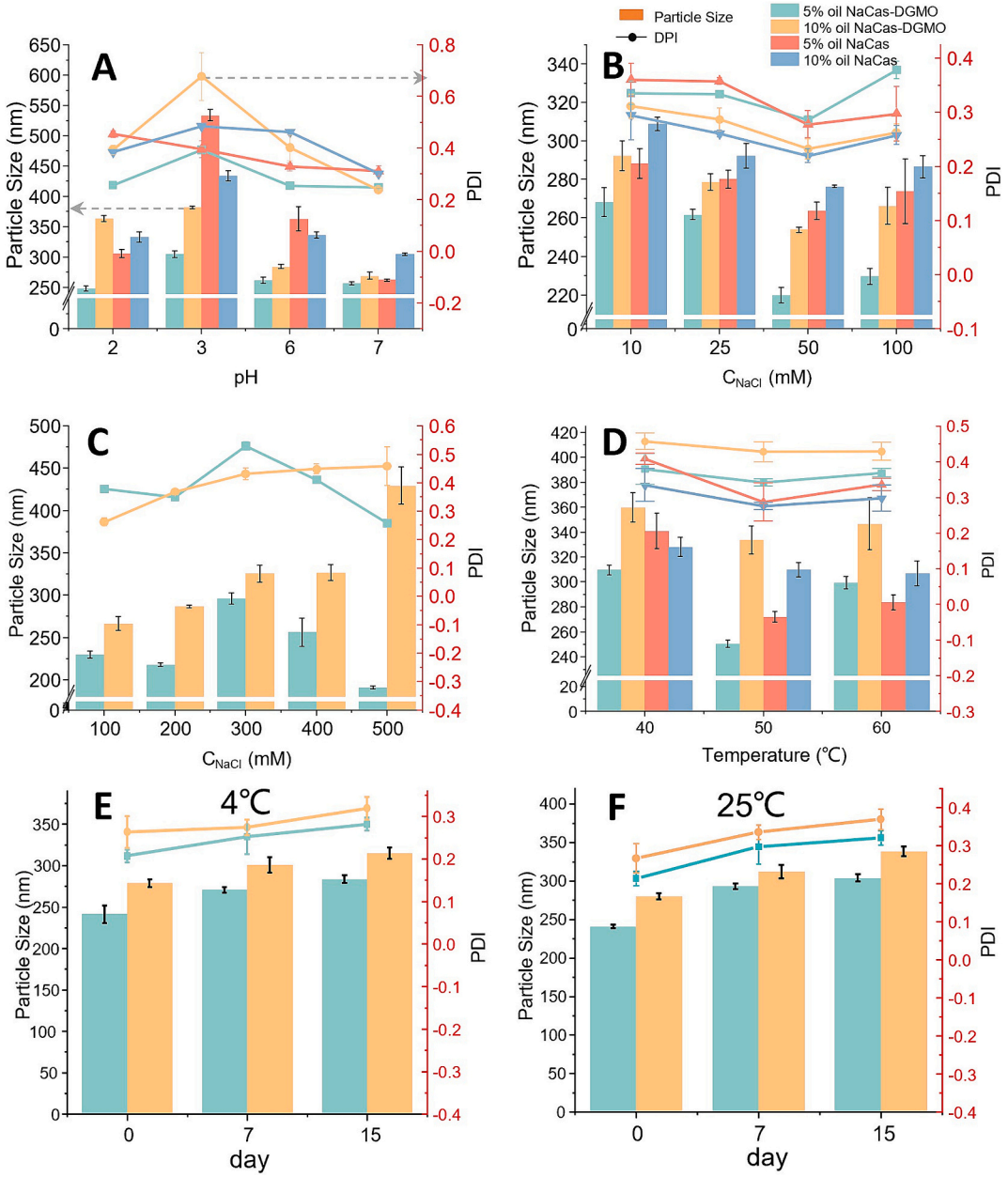

Fig. 2. The effect of (A) pH, (B&C) NaCl concentration and (D) temperature on the average particle size and polydispersity index (PDI) of Res-loaded emulsions stabilized by NaCas or NaCas-DGMO complex containing 5 % or 10 % rice brain oil (*v*/v). The 15-day storage stability of NaCas-DGMO complex stabilized emulsions with 5 % and 10 % oil at (E) 4 °C and (F) 25 °C. Data were expressed as mean ± SD ($n = 3$).

Yingxue et al., 2022). The PDI of 5 % and 10 % oil complex emulsion groups at pH 7 were <0.3, as well as particle size distribution at the nanoscale (256.5 ± 2.39 nm, 269 ± 5.93 nm, respectively), showing Res-loaded complex emulsions exhibited best stability and uniform dispersion at pH 7. Additionally, the average particle size of Res-loaded 10 % oil complex emulsion was always higher than 5 %-oil group. The correlation between oil content and particle size were consistent with the CLSM observation.

NaCl is commonly used to improve the flavor and extend the shelf life of food products, but it also alters the electrostatic interaction at the protein interface thereby affecting the stability of the emulsion. The ability of NaCl to modify the electrostatic interactions is crucial as it can either enhance or disrupt the emulsion's stability, depending on the concentration and the specific proteins involved. As shown in Fig. 2B, the particle size distribution of Res-loaded NaCas-DGMO emulsions at relatively low NaCl concentration (10–100 mM) ranged from 220 to 268.3 nm, yet those of NaCas-groups were from 236.7 to 288.2 nm. The smaller particle size in Res complex emulsion indicated that DGMO changed the surface charge properties of NaCas to avoid aggregation, improving the droplet's resistance to salt ionic strength. It was exhibited that the particle size and PDI values of different emulsions changed little as the increase of NaCl concentration from 10 mM to 100 mM. This observation suggested that within this specific concentration range, changes in ionic strength exerted little influence on the stability of Res-loaded NaCas-DGMO emulsions. The presence of DGMO in the Res-loaded NaCas emulsions appears to confer a degree of salt tolerance, as indicated by the minimal changes in particle size and polydispersity index (PDI) across the tested NaCl concentrations, suggesting a potential for improved emulsion stability under varying ionic conditions(Zhang, Zhang, Wang, & Wu, 2023).

Fig. 2C illustrated the effect of relatively high NaCl concentrations (100–500 mM) on the particle size and PDI of Res-loaded complex nanoemulsions. The particle size of the emulsions generally enlarged with the further increase of NaCl concentration, especially in 10 %-group. It was probably due to the electrostatic shielding effected of salt ions weakened the electrostatic repulsion between the droplets resulting in the aggregation (Kharat, Zhang, & McClements, 2018). Consistently, the PDI of Res-loaded complex emulsions generally above 0.3, suggesting the instability of both 5 % and 10 % emulsions. Therefore, the resistance to ionic strength of 5 %- and 10 %-oil emulsion were similar. Both were stable at relatively low concentration of NaCl (10–100 mM), while destabilized as the concentration of NaCl exceeded 100 mM.

Heat treatment is a typical process in the food industry. Food emulsions are subjected to a wide range of temperature environments during processing. Consequently, it was necessary to evaluate the stability of emulsions fabricated at varying temperatures. The effect of temperature on the stability of different emulsions was displayed in Fig. 2D. Generally, the particle size of both Res-loaded NaCas-DGMO and NaCas emulsions prepared at 40, 50 and 60 °C were in nanoscale with range of 250.4 ± 2.89 nm to 359.8 ± 11.63 nm. Compared with NaCas emulsions, the particle size of complex emulsions exhibited more pronounced variations in response to changes in the preparation temperature. Furthermore, the PDI of complex emulsions were slightly higher than that of NaCas emulsions, though they exhibited minimal fluctuations as the temperature increased from 40 °C to 60 °C. The results indicated that NaCas-DGMO emulsions displayed instability at relatively high temperatures.

Both emulsions (5 % and 10 % oil) were stored at 4 °C and 25 °C for 15 d, during which the particle size and PDI changed less (Fig. 2E and Fig. 2F). Among them, the particle size and PDI of emulsions were smaller at 4 °C than 25 °C. Generally, the smaller the particle size and the PDI, the better the emulsion stability. It showed that the low temperature conditions were more favorable for the storage of emulsions, although at 25 °C emulsions can still be stored stably. Consequently, the NaCas-DGMO emulsions were suitable for application at common temperature.

3.3. The encapsulation efficiency (EE) and micromorphology of NaCas-DGMO emulsions

Encapsulation efficiency (EE) is an important indicator for evaluating the performance of carrier systems. Res-loaded NaCas emulsions have been reported to achieve excellent emulsification and stability due to the formation of a stable interfacial layer where 90 % of the Res was loaded at the oil-water interface (Gong et al., 2022). It was speculated that the high EE was associated with large droplet size, which had an extensive oil-water interface. The EE of NaCas-DGMO complex emulsions with 0 %, 5 % oil and 10 % (v%) were 37 %, 72 %, and 92 % respectively as shown in Table 2. Indeed, the EE of the complex emulsions increased with the gradual increase of the oil volume. The EE values for the 5 % and 10 % oil NaCas-DGMO emulsions were higher than the EE of Res previously reported for NaCas and NaCas-dextran conjugates, which were 68 % and 83 %, respectively (Peñalva et al., 2018). The EE of the 10 % oil NaCas-DGMO complex emulsion reached 92 %, indicating that the emulsion system was a favorable and desirable carrier for Res delivery. Therefore, the subsequent morphological characterization, light stability, and biological evaluation were focused on the advantage of Res-loaded 10 % oil NaCas-DGMO emulsion. In subsequent discussions, these NaCas-DGMO complex emulsions are referred to as NaCas-DGMO emulsions with an oil content of 10 %. The TEM image in Fig. S1 depicted that the droplets were spherical and uniformly dispersed in the Res-loaded 10 % oil NaCas-DGMO emulsion, with particle size of approximately 200–300 nm. The results were consistent with the measurements of CLMS.

3.4. The photostability of Res-loaded emulsions

Res is a polyphenol with a conjugated double bond, rendering it susceptible to oxidation when exposed to light, ultimately compromising its biological activity. To address this, we investigated the photostability of Res in a NaCas-DGMO emulsion. A series of comparative experiments were conducted to assess the retention rate of Res within the NaCas-DGMO emulsion and control emulsions, both under light and dark conditions, over an extended period of time. The control groups included RC, RW, and RO, as detailed in the "Materials and Methods" section.

Fig. 3A presented the trends in the retention rates of Res in various media, including saline solution, rice bran oil, complex suspension, and NaCas-DGMO nanoemulsion, during a 21-day storage period at 4 °C under dark conditions. After this duration, the retention rates stood at 85.82 %, 94.80 %, 74.91 %, and 95.54 %, respectively. Notably, the NaCas-DGMO emulsion exhibited a significantly higher retention rate of Res compared to other groups, indicating that the addition of DGMO improved the protective effect of Res in emulsions. This might resulted from the NaCas-DGMO complex forming a superior interfacial protective layer on oil-water interface, effectively loading more Res though its photo-oxidation mainly occurred at the oil-water interface in the emulsion (Acharya et al., 2013; Gong et al., 2022), as well as shielding Res in the inner oil phase from the lighting environment (Puligundla, Mok, Ko, Liang, & Recharla, 2017). Comparatively, the retention rates of

Table 2
The encapsulation efficiency of Res-loaded NaCas-DGMO emulsion with 10 %, 5 %, and 0 % oil (v%). The measurements were repeated three times. Data were represented as mean ± SD.

	10 % oil Res-loaded NaCas-DGMO emulsion	5 % oil Res-loaded NaCas-DGMO emulsion	0 % oil Res-loaded NaCas-DGMO emulsion
Encapsulation efficiency	92% ± 2.1%	72% ± 0.4%	37% ± 0.59%

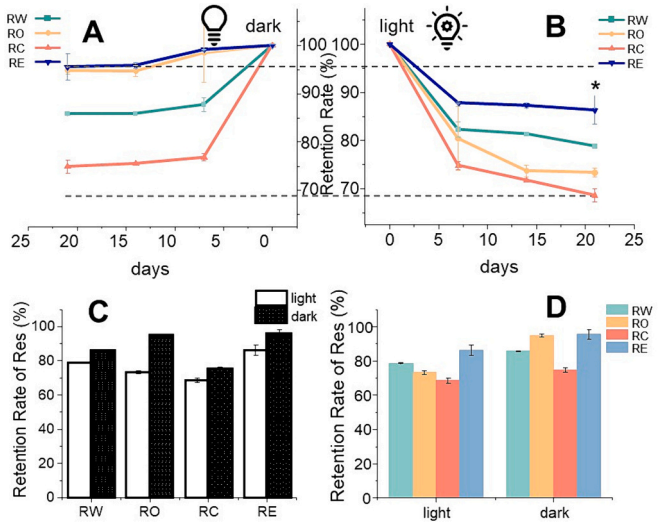

Fig. 3. The retention rates of Res in saline solution (RW), rice bran oil (RO), coarse emulsion (RC), and 10 % oil NaCas-DGMO nanoemulsion (RE) for 0, 7, 14, 21-day storage at 4 °C under (A) dark condition and (B) light condition. (C) The effect of light on the retention rates of Res in four groups after 21-day storage. (D) The discrepancy of the Res-retention rates from four groups after 21-day storage under light and dark condition. Data was represented as mean ± SD. All measurement were repeated at least three times. * Indicated statistically significant differences between RW, RO, RC and RE with one-way ANOVA ($p < 0.05$).

Res in saline, rice bran oil, coarse emulsion, and NaCas-DGMO emulsion after 21-day storage under light condition were 78.80 %, 73.32 %, 68.59 %, and 86.32 % (Fig. 3B), respectively, lower than the values at dark. The results indicated that light avoidance protected the Res in both solutions and emulsions from photochemical degradation (Fig. 3C). Furthermore, NaCas-DGMO emulsions enhanced photostability of Res and prolonged shelf-life of Res, even under light exposure (Fig. 3D).

3.5. Simulated gastrointestinal digestion

To further elucidate the potential digestive behavior and dynamic Res bioavailability of NaCas-DGMO emulsions, we employed an *in vitro* simulated gastrointestinal digestion model. Fig. 4A displayed the particle size and PDI of the original Res-loaded complex emulsion, digesta after simulated gastric fluid (SGF), and digesta after intestinal fluid (SIF) treatment. The original NaCas-DGMO emulsion showed relatively small particle size with the DPI value was <0.3, indicating the stability and uniform of emulsion. Afetr gastric digestion, there was minimal change in particle size, with a slight increase in PDI. This observation suggested that the presence of DGMO in combination with NaCas partially hindered the hydrolysis of NaCas by pepsin, thereby preserving the integrity of Res emulsion droplets during gastric digestion. Upon intestinal digestion, a significant increase in both particle size and PDI was observed (as depicted in Fig. 4A), indicating the destabilization of the NaCas-DGMO complex emulsion during the SIF stage. This destabilization can be attributed to the digestion of lipid droplets by lipase. Notably, this instability during intestinal digestion facilitated the release of Res in the intestine.

CLSM images supported these findings. As shown in Fig. 4B, Res-loaded NaCas-DGMO emulsion droplets, stained with Red Nile, were surrounded by a thin green layer after gastric digestion. This green layer likely represents FITC-stained protein, suggesting that the droplets remained partially intact after gastric digestion in the Res-emulsion (RE) group. In contrast, the droplets in the Res-NaCas-DGMO solution in the Res-control (RC) group appeared solely red, indicating complete hydrolysis of NaCas by pepsin during the 2-h gastric digestion. Consequently, the formation of NaCas-DGMO nanoparticles, absorbed onto

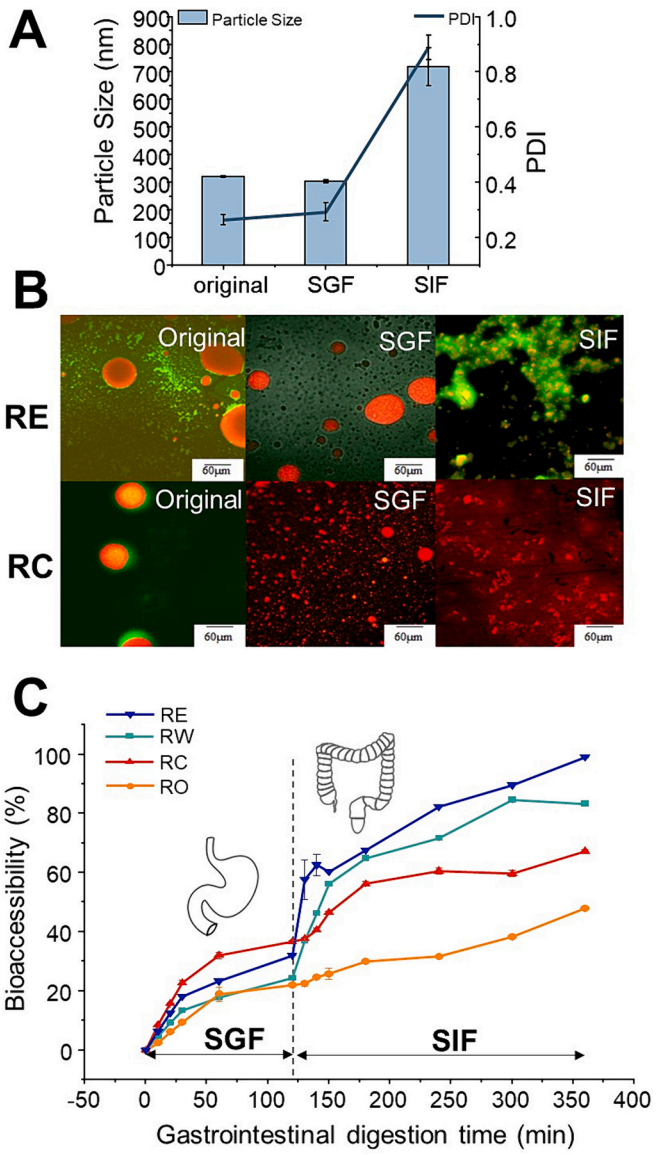

Fig. 4. (A) The particle size and PDI of Res-loaded NaCas-DGMO complex emulsion (n = 3). (B) CLSM images of Res-loaded NaCas-DGMO complex emulsion and Res/NaCas/DGMO/oil suspension after gastric and intestinal phase. (C) *In vitro* bioaccessibility of Res in different formulations after simulated gastrointestinal digestion (n = 3; SGF: Simulated gastric fluid SIF: Simulated intestinal fluid), including RE (0.5 mg/mL Res-loaded NaCas-DGMO emulsion), RW (0.5 mg/mL Res's water solution), RC (0.5 mg/mL Res/NaCas/DGMO/oil suspension), RO (0.5 mg/mL Res oil solution).

the oil droplets, impeded the hydrolysis of NaCas by pepsin and slowed down the release of Res (Zeng et al., 2023). After intestinal digestion, both the particle size of the Res-emulsion group significantly increased (Fig. 4A) and droplet flocculation occurred (Fig. 4B). This phenomenon maight be attributed to the emulsification of bile acids with oil and the aggregation of digesta caused by lipase digestion of oil droplets, consistent with previous research findings (Zeng et al., 2023).

The bioaccessibility of Res was difined as the proportion of Res released from the Res-contained food matrix into the aqueous phase in the intestinal lumen during ingestion and was available for absorption through intestinal membranes (Hu et al., 2023). Res-bioaccessibility were dertermined by collecting all mixed micelles at different digestive stage to calculate the percent of cumulative amount of Res in micelles to the total Res (Fig. 4C). As shown in Fig. 4C, during the simulated gastric fluid (SGF) stage, both the Res-containing NaCas-

DGMO emulsion (RE) and NaCas-DGMO solution (RC) consistently exhibited higher bioaccessibility compared to free Res, whether in oil (RO) or water (RW) solutions. This was likely attributed to the limited solubility of Res in both water and oil (Walle, 2011). These findings were in line with recent research demonstrating that complex emulsions could enhance Res bioaccessibility during *in vitro* simulated gastrointestinal digestion models (Zhang et al., 2023). Moreover, the NaCas-DGMO emulsion showed slightly lower bioaccessibility than the NaCas-DGMO solution, suggesting that the release of Res from the complex emulsion during the SGF stage was more controlled when compared to the complex solution group. After 2-h simulated gastric digestion, the Res-bioaccessibility of NaCas-DGMO emulsion was 32.11 %, while the NaCas-DGMO dispersion was 36.68 %. In the subsequent phase, when the digesta were mixed with simulated intestinal fluid (SIF) and incubated for an additional 4 h, the NaCas-DGMO emulsion group consistently maintained the highest Res bioaccessibility at all sampling points (Fig. 4C). By the end of the SIF stage, the Res bioaccessibility for RE had reached 99.11 %, whereas it was 67.2 % for RC, 47.88 % for RO, and 83.26 % for RW.

The results might be attributed to the protective effect of NaCas-DGMO composite particles in the RE group, allowing Res to undergo continuous and efficient emulsification due to the combined action of lipase and bile acid salts. In contrast, in the RC group where the NaCas-DGMO composite was absent, a portion of lipase and bile salts from SIF participated in the emulsification of the oil droplets, in which the solubility of Res was lower compared to water. Consequently, the content of Res in the mixed micellar layer was lower in the RC group than in the RE group, resulting in lower dynamic bioaccessibility. The RO group exhibited the lowest bioaccessibility due to limited solubility of Res in oil. On the other hand, the RW group showed relatively higher Res bioaccessibility at the end of simulated digestion (83.26 %), possibly because the process of simulated gastrointestinal digestion was accompanied by continuous dissolution of the Res powder.

3.6. *In vivo experiment*

Although *in vitro* simulated digestion has been a classical approach for evaluating the impact of food substrates, it falls short in accurately representing the complex nature of biological digestion. Digestion in living organisms is a dynamic process involving continuous metabolic communication between the intestine and the gut microbiome. This communication is facilitated by various entities, such as hormones, signaling molecules, and metabolites. Therefore, to investigate the effects of NaCas-DGMO complex nanoparticle encapsulation on the intestinal release and absorption of Res, as well as its impact on the gut microbiome, an *in vivo* digestive experiment on Sprague-Dawley (SD) rats was conducted.

3.6.1. *In vivo pharmacokinetic study of Res*

To evaluate the oral bioavailability of Res in different formulates, we performed a pharmacokinetic study with a dose of 10 mg/kg Res. The mean serum concentration-time curves of Res were presented in Fig. 5A, and the corresponding pharmacokinetic parameter, analyzed using Origin software, were summarized in Table 3. As shown, the Res-loaded NaCas-DGMO emulsion group exhibited a longer time to reach maximum concentration (T_{max}) compared to the free Res groups (RW and RO), as well as the RC group. This observation suggested that the combined delivery of NaCas-DGMO effectively retards the intestinal release of Res. Furthermore, the area under the curve from time 0 to 12 h ($AUC_{0–12}$) for Res in the emulsion group (6.38 ± 0.62 μg·h/mL, $p < 0.05$) was significantly greater than that in the RW, RO, and RC groups (4.79 ± 0.55, 1.73 ± 0.2, 2.06 ± 0.42 μg·h/mL, respectively), resulting in a 1.33-fold, 3.69-fold, and 3.1-fold increase in oral bioavailability, respectively. RW group exhibited the highest peak in Res's serum concentration at 0.5 h post-administration. This could be attributed to the rapid, uncontrolled release of Res from the water-based formulation compared to Res in oil, the complex suspension, and the emulsion. Similar findings have been reported in recent research regarding the time of Res serum peak concentration and the low bioavailability of oral Res-water solutions (Li et al., 2021; Peñalva et al., 2018; Wang et al., 2024). It would be due to the action of UDP-glucuronosyltransferase and sulfotransferases on Res, which primarily occurs in the liver and small intestine.

In the present study, the encapsulating of NaCas-DGMO complex nanoparticles prolonged Res plasma levels. The relatively high-Res's plasma levels were sustained for 6 h post administration in RE group, and the oral bioavailability increased 1.33 times than RW group. It was noteworthy that our findings surpassed those of previous research efforts in extending the time to reach the maximum serum concentration

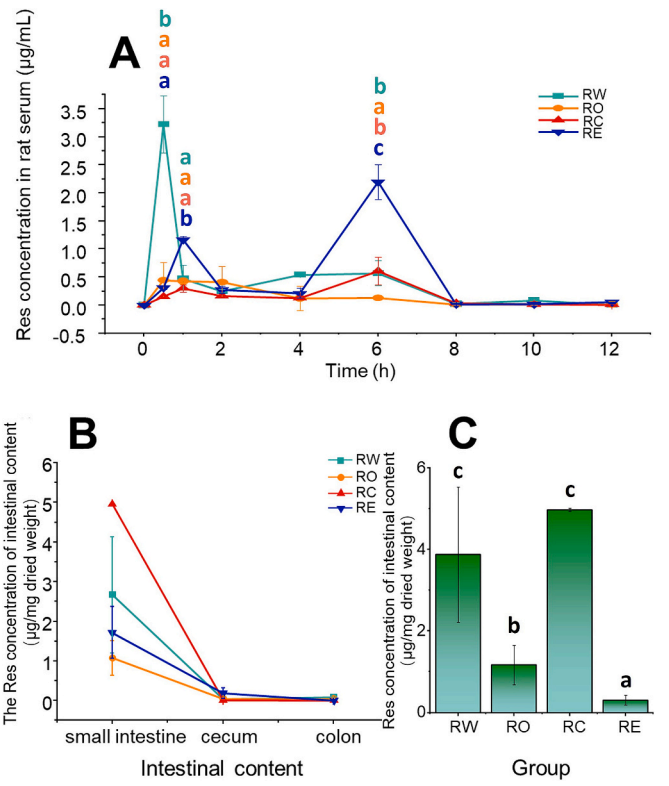

Fig. 5. (A) Mean serum concentration – time curves of Res after oral administration of RW, RO, RC and RE to rats at a dose of 10 mg/kg; (B) The Res concentration of varied intestinal segment, including small intestine, cecum and colon. The unit was μg per mg dried weight (μg/mg); (C) The total Res concentration of intestinal content. Data were represented as mean ± SD, $n = 7$. The lowercase letters represent statistical differences at the 0.05 level with one-way ANOVA between groups of RW, RO, RC and RE.

Table 3
Pharmacokinetic parameters for the oral administration of Res at a dose of 10 mg/kg. AUC, Area under the curve; C_{max}, Peak plasma concentration (The highest or peak level of a drug or medication that is observed in the plasma after it has been administered); T_{max}, Time to maximum plasma concentration. All values are expressed as mean ± SD ($n = 7$). *$p < 0.05$ *versus* RW.

	$AUC_{0–12}$	C_{max}(μg/mL)	T_{max}(h)
RW[a]	4.79 ± 0.55	3.22 ± 0.5	0.5
RO	1.73 ± 0.2	0.44 ± 0.01	0.5
RC	2.06 ± 0.42	0.6 ± 0.25	6
RE	6.38 ± 0.62*	2.19 ± 0.31	6

[a] RW refers to a solution with 0.5 mg/mL Res in saline, and RO refers to a solution with 0.5 mg/mL Res in rice brain oil. RE refers to the 0.5 mg/mL Res-loaded NaCas-DGMO emulsion containing 10 % oil (v%), RC refers to a 0.5 mg/mL Res-loaded NaCas-DGMO suspension with 10 % oil (v%).

(T_{max}). The T_{max} decreased to 55 % with Res/GA-PC prepared by Yingchao Li (Li et al., 2021), though the $AUC_{0–10}$ of Res in the Res/GA-PC group showed an increase of 2.49-fold. Rebeca Peñalva reported oral Res T_{max} increased to 1.8 h after encapsulation in Casein nanoparticles (Peñalva et al., 2018). Thus, Res loaded NaCas-DGMO emulsion delivery effectively control the intestinal release of Res, so that the serum concentration of Res kept at a relatively high level over a longer term, which further increase the absorption of Res.

3.6.2. *In vivo intestinal tract residuals of Res*

In order to visually elucidate the intestinal release and absorption of Res in different formulates. We quantified Res in the intestinal contents of different intestinal segments in four groups of rats at 12.5 h post oral administration. As shown in Fig. 5B, in four groups, the amount of Res in small intestinal contents was higher than that in the cecal contents and colonic contents, indicating that the release of Res from the food matrix occurred mainly in the small intestine. Further, we analyzed the total amount of Res in the intestinal contents of rats (Fig. 5C). It was found

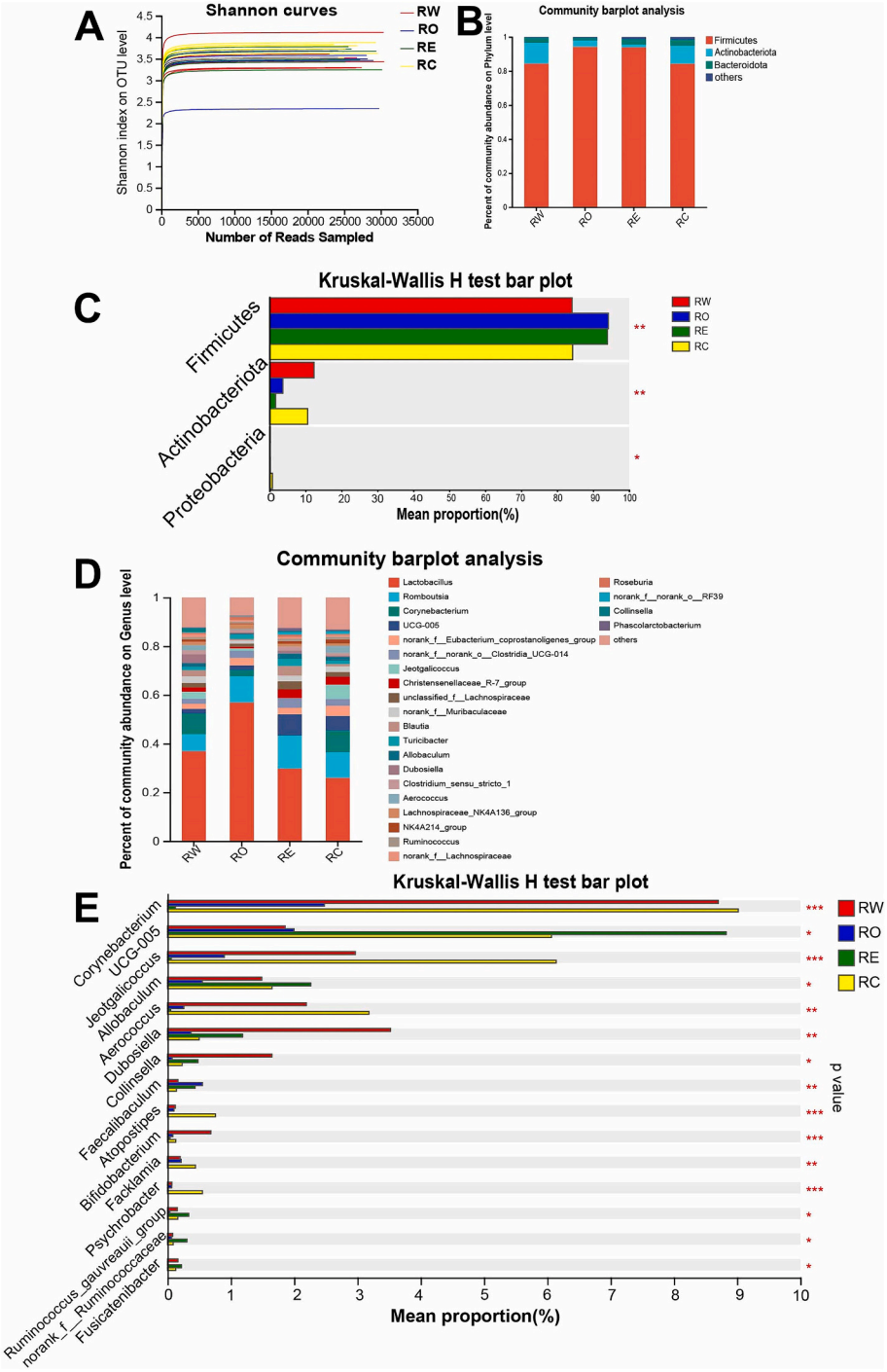

Fig. 6. Shannon curves (A), community composition analysis on phylum(B) and genus level (D) for gut microbiota within the colonic content samples from four experimental groups: RW (Resveratrol saline), RO (Resveratrol oil), RE (Resveratrol loaded complex emulsion), and RC (Resveratrol complex suspension). Significantly varied bacteria on phylum (C) and genus (E) when comparing the four aforementioned groups. p values were obtained through Kruskal-Wallis H test. n = 3, *$0.01<p \leq 0.05$, ** $0.001 <p \leq 0.01$, *** $p \leq 0.001$.

that the total amount of Res in the intestinal contents of the rats orally administrated Res's emulsion (RE) was significantly lower than that of the other three groups. This suggested that the proportion of unabsorbed Res in the intestinal tract of the RE group was the lowest after 12.5 h post oral administration, and conversely, the amount of Res absorbed into the body circulation was the highest. This was in accordance with the results of serum Res. Therefore, the NaCas-DGMO emulsion delivery system can effectively achieve the controlled intestinal release of Res and enhance the bioavailability of Res.

As the emulsion delivery system holds the potential to enhance the bioavailability of Res, what effect does the NaCas-DGMO complex nanoparticles have on the intestinal metabolome of rats? We subsequently investigated the intestinal metabolite composition of four groups of rats basing on NMR technique. Fig. S2 were typical NMR spectra of colonic contents from four groups of rats. Initially, we analyzed the metabolic profiles of small intestine, cecum, and colonic contents from each group of rats using a multivariate approach. As illustrated in Fig. S3, the principal component analysis (PCA) score plots demonstrated that there was no noticeable distinction in the nuclear magnetic resonance (NMR)-based metabolic profiles of the small intestine, cecum, and colon contents. This indicated that there was no significant intergroup differentiation. This suggested that single dose of varied formulated Res did not induce changes of rat intestinal metabolism post oral administration 12.5 h, which may be due to the low dose of Res intervention. To further explore the changes in rat intestinal metabolism induced by varied formulated Res, we listed relative amounts of several metabolites based on NMR peak area such as, butyrate acid, formic acid in the intestinal contents of different intestinal segments (Fig. S4). It was found that the amount of butyric acid in the small intestinal contents of rats in the RE group was significantly higher than that in the other groups. Butyric acid in the intestine is metabolized by intestinal flora, and butyric acid not only provides energy for intestinal epithelial cells, which maintained the integrity of the intestinal barrier, but also improves intestinal immune function (Tan et al., 2014). The elevated butyric acid content in the intestines of rats orally administered with Res complex emulsion was likely due to the action of butyric acid-producing intestinal flora (den Besten et al., 2013; Tan et al., 2014).

3.6.3. Modification of gut microbiota

To elucidate the alterations in gut microbiota induced by the different Res formulations, we analyzed the microbial composition of colonic contents. Particularly, the impact of emulsion and non-emulsion formulations on gut microbial *in vivo* regulation was focused, so the groups of RE and RC were chosen in this section. As depicted in Fig. 6A, the Shannon rarefaction curve for all samples exhibited a flat profile, signifying that sequencing data coverage was sufficient to encompass nearly all microbial information, indicating our data robust and reliable. While no significant disparities were observed in the OTU-level richness and α-diversity of colonic contents among the four experimental groups (results not shown), a noteworthy finding emerged concerning the Firmicutes-to-Bacteroidetes ratio, two dominant phyla (Fig. 6B). The Res-oil and Res-emulsion groups exhibited a significantly higher Firmicutes-to-Bacteroidetes ratio compared to the other two groups (Fig. 6C). The high Firmicutes-to-Bacteroidetes ratio in terms of their abundance were closely relative with the obesity risk caused both by internal and external factors in vast previous reports (Nicholson et al., 2012), which played a key role in regulating lipid and glucose metabolism. The elevated F/B ratio could potentially be attributed to the dietary oil intake by rats in the RO and RE groups, with a notable emphasis on the RE group, where the oil was encapsulated within complex nanoparticles, facilitating its absorption by intestinal epithelial cells. From Fig. 6D, the *Lactobacillus* was the dominant bacterial community at the level of genus as prior research reported. (Zeng et al., 2023) No significant variations in Lactobacillus abundance were detected among the different treatment groups. Nevertheless, encapsulation of Res resulted in a significant increase in the abundance of several bacterial genera, including *Ruminococcus_gauvreauii_group* ($p = 0.038$), *Ruminococcus UCG-005* ($p = 0.048$), *Fusicatenibacter* ($p = 0.024$) (Fig. 6E). Among these, *Ruminococcus_gauvreauii_group, Ruminococcus UCG-005* have been linked to intestinal acetate production in previous research. (Lin et al., 2016) *Fusicatenibacter* was also a kind of short fatty acids producing bacterial genus (Samuel et al., 2008). The results showed that the encapsulation shifted the bacterial community towards a more health-promoting profile.

Having discussed the variations in intestinal flora induced by the four different treatments (including Res's suspensions in water and oil, composite nanoemulsions of Res, and Res-NaCas-DGMO-oil suspensions), we further explored the effects of CaNas-DGMO nanoparticle encapsulation on intestinal flora by specifically comparing the abundance of intestinal flora between the latter two groups at different taxonomic levels.

It was noteworthy that the abundance of *Erysipelotrichaceae* and *Lachnospiraceae* in the RE group was significantly higher than that of the RC group at the family level (Fig. 7A). *Erysipelotrichaceae* was a butyric acid-producing bacterium that produced butyric acid, which was the main energy donor for intestinal epithelial cells and improved the immune function of the intestine. In a recent Spinal cord injury study, elevated levels of family-level bacterial *Erysipelotrichaceae* were positively correlated with the treatment of Res (He et al., 2022). Elevated levels of *Erysipelorichaceae* in the RE group indicated that NaCas-encapsulation of Res by DGMO composite nanoparticles enhanced the *in vivo* bioactivity of Res and promoted intestinal health. Moreover, *Lanchnoapiraceae* was thought as an essential member of the heathy fecal microbiota in the human intestine and was benefit to the human health (Reeves, Koenigsknecht, Bergin, & Young, 2012).

As illustrated in Fig. 7B, at the genus level, bacteria such as *Blautia*, *Feacalibaculum*, and *Ruminococcaceae* exhibited significantly higher abundances in the RE group compared to the RC group. Notably, *Blautia* is known to produce acetate, serving as a secondary energy source for intestinal epithelial cells while also inhibiting pathogenic bacteria, thereby exerting anti-inflammatory effects (Kimura et al., 2013; Li et al., 2022). Conversely, the relative abundance of certain genera, including *Corynebacterium* and *Jeotgalicoccus*, significantly decreased. Of these, *Corynebacterium* was highly pathogenic and could lead to diphtheria (Kalt et al., 2018). The above analysis showed that Res-encapsulation increased the proportion of beneficial bacteria and shifted the bacterial community to health for host.

4. Conclusion

The research aimed to investigate the impact of the NaCas/DGMO complex emulsion on the stability, bioaccessibility, and bioavailability of resveratrol, as well as its potential modulation of the gut microbiota. The emulsion exhibited an 92 % encapsulation efficiency and demonstrated remarkable stability against pH variations, ionic strength, and light exposure. *In vitro* digestion studies demonstrated that the emulsion enhanced the bioaccessibility of resveratrol. This finding was also supported by *in vivo* rat pharmacokinetics, which indicated improved bioavailability and a prolonged T_{max} of 6 h post-treatment. The study also examined the impact of encapsulation on intestinal metabolism and microbiota, observing a beneficial shift in gut microbiota despite no significant changes in metabolism detected by NMR. It indicated that further investigation over an extended period may elucidate additional insights into the emulsion's metabolic effects. Collectively, the research demonstrated the potential of nano-emulsions as a valuable tool for the food industry, offering a protective and targeted delivery system for bioactive ingredients, and proposed a novel methodology for evaluating the biological efficacy of such systems.

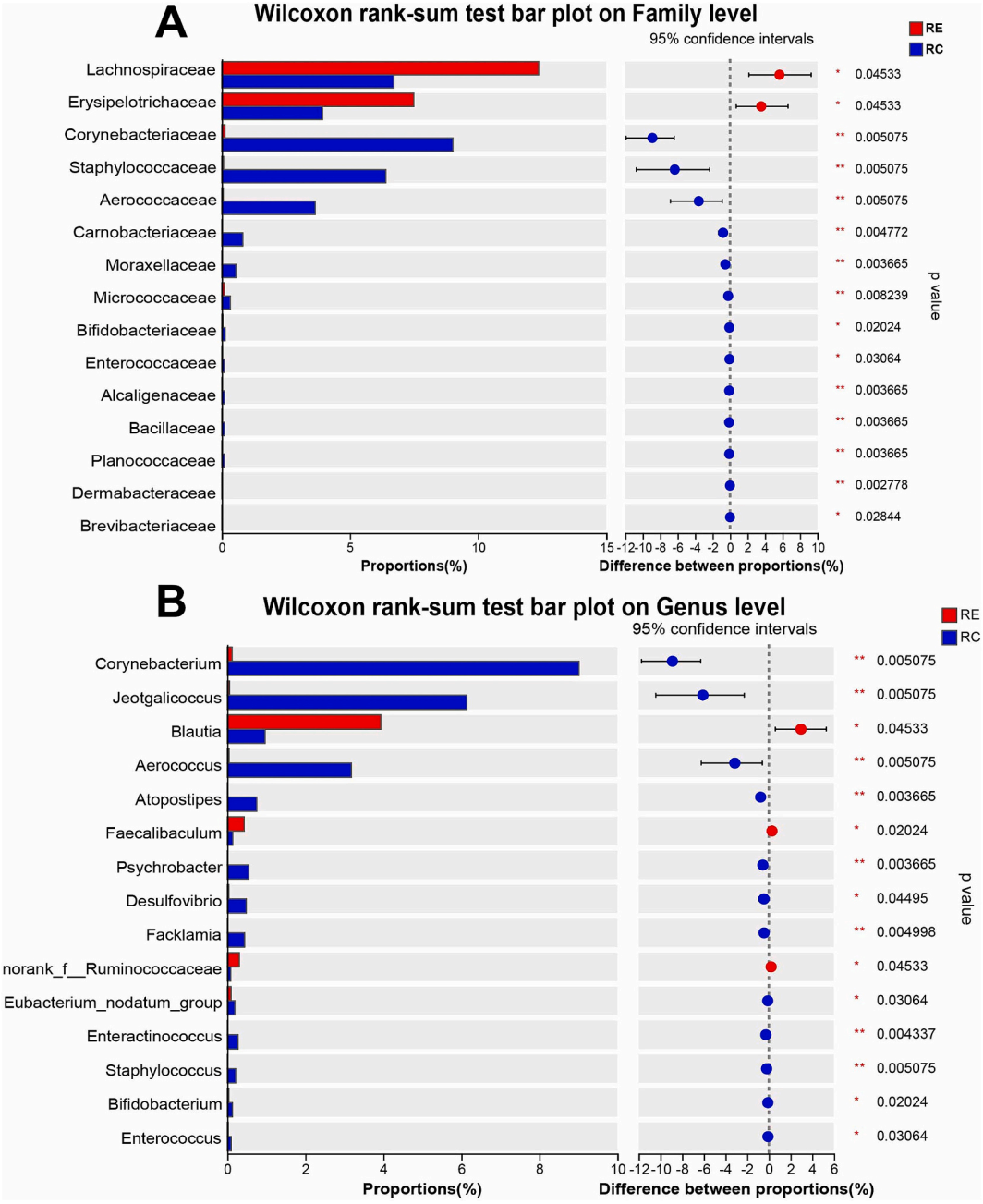

Fig. 7. Significantly varied bacteria on family (A) and genus (B) when comparing the RE group and RC group. *p* values were obtained through Wilcoxon rank-sum test. n = 3, *$0.01 < p \leq 0.05$, ** $0.001 < p \leq 0.01$.

CRediT authorship contribution statement

Hong Lin: Writing – review & editing, Writing – original draft, Funding acquisition, Conceptualization. **Huan Chen:** Writing – original draft, Investigation. **Siqi Wang:** Investigation, Data curation. **Junbo He:** Data curation, Conceptualization. **Weinong Zhang:** Writing – review & editing, Supervision, Conceptualization.

Declaration of competing interest

The authors declare that they have no known competing financial interests or personal relationships that could have appeared to influence the work reported in this paper.

Data availability

Data will be made available on request.

Acknowledgment

This work was supported by the National Natural Science Foundation of China (Grant Nos. 32101967), Open Project Program of MOE Key Laboratory for Deep Processing of Major Grain and Oil (Wuhan Polytechnic University)(2020JYBQGDKFB06), Special Project of Central Guide to Local Science and Technology Development (Innovation platform construction for food green processing technology and intelligent equipment) (2022BGE247).

Appendix A. Supplementary data

Supplementary data to this article can be found online at https://doi.org/10.1016/j.fochx.2024.101724.

References

Acharya, D. P., Sanguansri, L., & Augustin, M. A. (2013). Binding of resveratrol with sodium caseinate in aqueous solutions. *Food Chemistry, 141*(2), 1050–1054. https://doi.org/10.1016/j.foodchem.2013.03.037

Ai, Y., Fang, F., Zhang, L., & Liao, H. (2022). Antimicrobial activity of oregano essential oil and resveratrol emulsions co-encapsulated by sodium caseinate with polysaccharides. *Food Control, 137*, Article 108925. https://doi.org/10.1016/j.foodcont.2022.108925

Andres-Lacueva, C., Macarulla, M. T., Rotches-Ribalta, M., Boto-Ordóñez, M., Urpi-Sarda, M., Rodríguez, V. M., & Portillo, M. P. (2012). Distribution of resveratrol metabolites in liver, adipose tissue, and skeletal muscle in rats fed different doses of this polyphenol. *Journal of Agricultural and Food Chemistry, 60*(19), 4833–4840. https://doi.org/10.1021/jf3001108

den Besten, G., van Eunen, K., Groen, A. K., Venema, K., Reijngoud, D. J., & Bakker, B. M. (2013). The role of short-chain fatty acids in the interplay between diet, gut microbiota, and host energy metabolism. *Journal of Lipid Research, 54*(9), 2325–2340. https://doi.org/10.1194/Jlr.R036012

Chen, J., Zhang, J., Xu, Z., Kong, B., Wang, H., Tang, J., … Li, X. (2023). Resveratrol promotes interfacial adsorption behaviour and retards protein-lipid co-oxidation of whey protein isolate stabilised O/W emulsions. *Food Hydrocolloids, 144*, Article 109010. https://doi.org/10.1016/j.foodhyd.2023.109010

Dima, C., Assadpour, E., Dima, S., & Jafari, S. M. (2020). Bioavailability of nutraceuticals: Role of the food matrix, processing conditions, the gastrointestinal tract, and nanodelivery systems. *Comprehensive Reviews in Food Science and Food Safety, 19*(3), 954–994. https://doi.org/10.1111/1541-4337.12547

Gausuzzaman, S. A. L., Saha, M., Dip, S. J., Alam, S., Kumar, A., Das, H., … Reza, H. M. (2022). A QbD approach to design and to optimize the self-emulsifying resveratrol-phospholipid complex to enhance drug bioavailability through lymphatic transport. *Polymers (Basel), 14*(15). https://doi.org/10.3390/polym14153220

Ghorbanzade, T., Jafari, S. M., Akhavan, S., & Hadavi, R. (2017). Nano-encapsulation of fish oil in nano-liposomes and its application in fortification of yogurt. *Food Chemistry, 216*, 146–152. https://doi.org/10.1016/j.foodchem.2016.08.022

Gong, T., Chen, B., Hu, C. Y., Guo, Y. R., Shen, Y. H., & Meng, Y. H. (2022). Resveratrol inhibits lipid and protein co-oxidation in sodium caseinate-walnut oil emulsions by reinforcing oil-water interface. *Food Research International, 158*, Article 111541. https://doi.org/10.1016/j.foodres.2022.111541

He, N., Shen, G., Jin, X., Li, H., Wang, J., Xu, L., … Wang, L.-L. (2022). Resveratrol suppresses microglial activation and promotes functional recovery of traumatic spinal cord via improving intestinal microbiota. *Pharmacological Research, 183*, Article 106377. https://doi.org/10.1016/j.phrs.2022.106377

Hu, Y., Lin, Q., Zhao, H., Li, X., Sang, S., McClements, D. J., … Qiu, C. (2023). Bioaccessibility and bioavailability of phytochemicals: Influencing factors, improvements, and evaluations. *Food Hydrocolloids, 135*, Article 108165. https://doi.org/10.1016/j.foodhyd.2022.108165

Huang, S., He, J., Cao, L., Lin, H., Zhang, W., & Zhong, Q. (2020). Improved physicochemical properties of curcumin-loaded solid lipid nanoparticles stabilized by sodium caseinate-lactose maillard conjugate. *Journal of Agricultural and Food Chemistry, 68*(26), 7072–7081. https://doi.org/10.1021/acs.jafc.0c01171

Joseph, A., Balakrishnan, A., Shanmughan, P., Maliakel, B., & Illathu Madhavamenon, K. (2022). Micelle/hydrogel composite as a "Natural Self-Emulsifying Reversible Hybrid Hydrogel (N'SERH)" enhances the oral bioavailability of free (unconjugated) resveratrol. *ACS Omega, 7*(15), 12835–12845. https://doi.org/10.1021/acsomega.2c00116

Kalt, F., Schulthess, B., Sidler, F., Herren, S., Fucentese, S. F., Zingg, P. O., … Achermann, Y. (2018). Corynebacterium species rarely cause orthopedic infections. *Journal of Clinical Microbiology, 56*(12). https://doi.org/10.1128/jcm.01200-18

Kharat, M., Zhang, G., & McClements, D. J. (2018). Stability of curcumin in oil-in-water emulsions: Impact of emulsifier type and concentration on chemical degradation. *Food Research International, 111*, 178–186. https://doi.org/10.1016/j.foodres.2018.05.021

Kimura, I., Ozawa, K., Inoue, D., Imamura, T., Kimura, K., Maeda, T., … Tsujimoto, G. (2013). The gut microbiota suppresses insulin-mediated fat accumulation via the short-chain fatty acid receptor GPR43. *Nature Communications, 4*, 1829. https://doi.org/10.1038/ncomms2852

Li, Y., Qin, C., Dong, L., Zhang, X., Wu, Z., Liu, L., … Liu, L. (2022). Whole grain benefit: Synergistic effect of oat phenolic compounds and β-glucan on hyperlipidemia via gut microbiota in high-fat-diet mice. *Food & Function, 13*(24), 12686–12696. https://doi.org/10.1039/d2fo01746f

Li, Y., Zhang, R., Zhang, Q., Luo, M., Lu, F., He, Z., … Zhang, T. (2021). Dual strategy for improving the Oral bioavailability of resveratrol: Enhancing water solubility and inhibiting glucuronidation. *Journal of Agricultural and Food Chemistry, 69*(32), 9249–9258. https://doi.org/10.1021/acs.jafc.1c02602

Lin, H., An, Y., Hao, F., Wang, Y., & Tang, H. (2016). Correlations of fecal metabonomic and microbiomic changes induced by high-fat diet in the pre-obesity state. *Scientific Reports, 6*. https://doi.org/10.1038/srep21618

Lin, H., Fu, S., Hu, C., Zhang, W., & He, J. (2024). Characterization, interfacial rheology, and storage stability of Pickering emulsions stabilized by complex of whey protein isolate fiber and zein derived from micro-endosperm maize. *International Journal of Biological Macromolecules, 261*, Article 129948. https://doi.org/10.1016/j.ijbiomac.2024.129948

Liu, K., Liu, Y., Lu, J., Liu, X., Hao, L., & Yi, J. (2023). Nanoparticles prepared by polysaccharides extracted from Biyang floral mushroom loaded with resveratrol: Characterization, bioactivity and release behavior under in vitro digestion. *Food Chemistry, 426*, Article 136612. https://doi.org/10.1016/j.foodchem.2023.136612

Mora-Gutierrez, A., Attaie, R., de Gonzalez, M. T. N., Jung, Y. S., & Marquez, S. A. (2020). Interface compositions as determinants of resveratrol stability in nanoemulsion delivery systems. *Foods, 9*(10). https://doi.org/10.3390/foods9101394

Murray, B. S. (2002). Interfacial rheology of food emulsifiers and proteins. *Current Opinion in Colloid & Interface Science, 7*(5–6), 426–431. doi:Pii S1359-0294(02)00077-8 https://doi.org/10.1016/S1359-0294(02)00077-8.

Nicholson, J. K., Holmes, E., Kinross, J., Burcelin, R., Gibson, G., Jia, W., & Pettersson, S. (2012). Host-gut microbiota metabolic interactions. *Science, 336*(6086), 1262–1267. https://doi.org/10.1126/science.1223813

Peñalva, R., Morales, J., González-Navarro, C. J., Larrañeta, E., Quincoces, G., Peñuelas, I., & Irache, J. M. (2018). Increased Oral bioavailability of resveratrol by its encapsulation in casein nanoparticles. *International Journal of Molecular Sciences, 19*(9), 2816.

Puligundla, P., Mok, C., Ko, S., Liang, J., & Recharla, N. (2017). Nanotechnological approaches to enhance the bioavailability and therapeutic efficacy of green tea polyphenols. *Journal of Functional Foods, 34*, 139–151. https://doi.org/10.1016/j.jff.2017.04.023

Reeves, A. E., Koenigsknecht, M. J., Bergin, I. L., & Young, V. B. (2012). Suppression of *Clostridium difficile* in the gastrointestinal tracts of germfree mice inoculated with a murine isolate from the family Lachnospiraceae. *Infection and Immunity, 80*(11), 3786–3794. https://doi.org/10.1128/iai.00647-12

Sahraeian, S., Rashidinejad, A., & Golmakani, M.-T. (2024). Recent advances in the conjugation approaches for enhancing the bioavailability of polyphenols. *Food Hydrocolloids, 146*, Article 109221. https://doi.org/10.1016/j.foodhyd.2023.109221

Samuel, B. S., Shaito, A., Motoike, T., Rey, F. E., Backhed, F., Manchester, J. K., … Gordon, J. I. (2008). Effects of the gut microbiota on host adiposity are modulated by the short-chain fatty-acid binding G protein-coupled receptor, Gpr41. *Proceedings of the National Academy of Sciences of the United States of America, 105*(43), 16767–16772. https://doi.org/10.1073/pnas.0808567105

Sessa, M., Balestrieri, M. L., Ferrari, G., Servillo, L., Castaldo, D., D'Onofrio, N., … Tsao, R. (2014). Bioavailability of encapsulated resveratrol into nanoemulsion-based delivery systems. *Food Chemistry, 147*, 42–50. https://doi.org/10.1016/j.foodchem.2013.09.088

Shang, L. C., Wang, Y., Ren, Y. Y., Ai, T. Y., Zhou, P. Y., Hu, L., … Li, B. (2020). Gastric emptying characteristics of konjac glucomannan with different viscosity and its effects on appetite regulation. *Food & Function, 11*(9), 7596–7610. https://doi.org/10.1039/d0fo01104e

Shi, L., Cheng, Y., Jia, C., Lin, H., Zhang, W., & He, J. (2024). Stable complex of sodium caseinate and hexaglycerol monooleate with improved oil-in-water emulsion stability and curcumin encapsulation. *Food Biophysics, 19*(2), 321–333. https://doi.org/10.1007/s11483-024-09828-8

Shi, Z. H., Chen, H., He, J. B., Zhang, W. N., & Lin, H. (2024). The addition of resveratrol-loaded emulsions to yogurts: Physicochemical characterization, in vitro bioaccessibility and NMR-based nutritional profiles. *Foods, 13*(3). https://doi.org/10.3390/foods13030426. ARTN 426.

Silva, P. M., Gonçalves, C., Pastrana, L. M., Coimbra, M. A., Vicente, A. A., & Cerqueira, M. A. (2023). Recent advances in oral delivery systems of resveratrol: Foreseeing their use in functional foods. *Food & Function, 14*(23), 10286–10313. https://doi.org/10.1039/d3fo03065b

Tamjidi, F., Shahedi, M., Varshosaz, J., & Nasirpour, A. (2013). Nanostructured lipid carriers (NLC): A potential delivery system for bioactive food molecules. *Innovative Food Science & Emerging Technologies, 19*, 29–43. https://doi.org/10.1016/j.ifset.2013.03.002

Tan, J., McKenzie, C., Potamitis, M., Thorburn, A. N., Mackay, C. R., & Macia, L. (2014). The role of short-chain fatty acids in health and disease. *Advances in Immunology, 121*(121), 91–119. https://doi.org/10.1016/B978-0-12-800100-4.00003-9

Walle, T. (2011). Bioavailability of resveratrol. In O. Vang, & D. K. Das (Eds.), *Vol. 1215. Resveratrol and health* (pp. 9–15).

Wang, L., Jia, W., Yang, Q., Cai, H., & Zhao, X. (2024). Casein nanoparticles as oral delivery carriers for improved bioavailability and hypoglycemic activity of apigenin. *Food Hydrocolloids, 146*, Article 109194. https://doi.org/10.1016/j.foodhyd.2023.109194

Wenzel, E., Soldo, T., Erbersdobler, H., & Somoza, V. (2005). Bioactivity and metabolism of trans-resveratrol orally administered to Wistar rats. *Molecular Nutrition & Food Research, 49*(5), 482–494. https://doi.org/10.1002/mnfr.200500003

Wu, Y. B., Wan, J. W., Choe, U., Pham, Q., Schoene, N. W., He, Q., … Wang, T. T. Y. (2019). Interactions between food and gut microbiota: Impact on human health. In M. P. Doyle, & D. J. McClements (Eds.), *Vol. 10. Annual Review of Food Science and Technology* (pp. 389–408).

Yin, X., Dong, H., Cheng, H., Ji, C., & Liang, L. (2022). Sodium caseinate particles with co-encapsulated resveratrol and epigallocatechin-3-gallate for inhibiting the oxidation of fish oil emulsions. *Food Hydrocolloids, 124*, Article 107308. https://doi.org/10.1016/j.foodhyd.2021.107308

Yingxue, C., Menglu, W., & Junbo, H. E. (2022). Preparation of decaglycerol monooleate-sodium caseinate complex and stabilization for citral. *Modern Food Science and Technology, 38*(12), 74–83.

Zeng, Z., Deng, S., Liu, Y., Li, C., Fang, Z., Hu, B., … Liu, Y. (2023). Targeting transportation of curcumin by soybean lipophilic protein nano emulsion: Improving

its bioaccessibility and regulating intestinal microorganisms in mice. *Food Hydrocolloids, 142*, Article 108781. https://doi.org/10.1016/j.foodhyd.2023.108781

Zhang, J., Zhang, X., Wang, Q., & Wu, C. (2023). Changes of physicochemical properties and bioactivities of resveratrol-loaded core–shell biopolymer nanoparticles during in vitro gastrointestinal digestion. *Food Chemistry, 424*, Article 136444. https://doi.org/10.1016/j.foodchem.2023.136444

Zhu, P., He, J., Huang, S., Han, L., Chang, C., & Zhang, W. (2021). Encapsulation of resveratrol in zein-polyglycerol conjugate stabilized O/W nanoemulsions: Chemical stability, in vitro gastrointestinal digestion, and antioxidant activity. *LWT, 149*, Article 112049. https://doi.org/10.1016/j.lwt.2021.112049